Imaging of the Posterior Skull Base

Joici Job, MD, Barton F. Branstetter IV, MD*

KEYWORDS

• Skull base • Cranial nerves • Foramen magnum • Jugular fossa

KEY POINTS

- A dedicated skull base protocol is critical to evaluation of poster skull base anomalies.
- Knowledge of normal lower cranial nerve anatomy allows proper radiologic assessment of posterior fossa pathology.
- Disease of the posterior skull base often presents with symptoms from progression into surrounding regions.

INTRODUCTION

Accurate detection of underlying pathology involving the posterior skull base requires an understanding of normal and normal variant anatomy, especially the course of the lower cranial nerves (CNs), IX through XII. This helps identify and classify common clinical presentations based on location of pathologic involvement.

Posterior skull base pathology can be grouped into 4 major categories: trauma/acquired, neoplastic, infectious, and vascular. This article is organized in accordance with this scheme. Abnormalities of the posterior skull base frequent present with extension of pathology beyond the skull base, both intracranially and caudally, to involve the suprahyoid neck.

Imaging protocols for the posterior skull base should be tailored to the individual patient to optimize characterization of the abnormality and provide relevant information for treatment planning.

PROTOCOLS

At the authors' institution, every skull base MRI is individually tailored to the patient based on prior imaging and clinical history. The key piece of information provided to the technologists is the anatomic extent of imaging. This allows using smaller fields of view and reducing overall imaging time. The default pulse sequences for the skull base protocol are

Full brain
- T1-weighted sagittal
- Diffusion-weighted imaging axial
- Fluid-attenuated inversion recovery (FLAIR) axial

Skull base region of interest
- T1-weighted axial and coronal
- T2-weighted (fat saturated) axial and coronal
- Contrast-enhanced T1-weighted (fat saturated) axial and coronal
- 3-D spoiled gradient (acquired in axial with sagittal and coronal reformatted images)

Some considerations for further tailoring posterior skull base protocols include

- Neurovascular compression: 3-plane thin-section steady-state free-precession imaging (SSFP) to delineate lower CN course and better characterize the culprit vessel (artery/vein), point of contact, and/or deformity.
- Contrast-enhanced FLAIR sequences to improve sensitivity for leptomeningeal disease

Department of Radiology, University of Pittsburgh Medical Center, University of Pittsburgh, 200 Lothrop Street, Pittsburgh, PA 15213, USA
* Corresponding author.
E-mail address: branbf@UPMC.EDU

Radiol Clin N Am 55 (2017) 103–121
http://dx.doi.org/10.1016/j.rcl.2016.08.002

- Contrast-enhanced SSFP sequences to characterize CN involvement (particularly useful when there is extension of disease into the cavernous sinuses.)
- Automated volume measurements on both CT and MRI are useful on serial follow-ups in the post-treatment setting.
- In addition to standard coronal and sagittal reconstructions in bony and soft tissue algorithms, 3-D surface rendering can be helpful for surgical planning on CT. For example, when Eagle syndrome is suspected, these reconstructions may better delineate the course of the styloid process relative to the faucial tonsil.[1]

POSTERIOR SKULL BASE ANATOMY AND EMBRYOLOGY

The clivus forms the anterior aspect of the posterior skull base from fusion of the basisphenoid and basiocciput at the spheno-occipital synchondrosis (**Fig. 1**). The craniocaudal extent of the posterior skull base is from the foramen magnum inferordorsally to the dorsum sellae superoventrally.[2] The laterosuperior portion of the posterior skull base is formed by the posterior surface of the petrous portion of the temporal bone and the mastoid portion of the temporal bone.[3]

The condylar portion of the occipital bone forms the lateral posterior skull base inferiorly. The junction between the petrous portions of the temporal bone and the occipital bone is the petroccipital suture/fissure[4] (see **Fig. 1**). The posterior portion of the posterior skull base is formed by the occipital bone. The petrous ridge of the temporal bone divides the central skull base from the posterior skull base and is the attachment for the fixed edge of the tentorium cerebelli.[5]

Embryologically, there are 4 major ossification centers form the foramen magnum: the supraoccipital, basioccipital, and paired exoccipital. Although the posterior skull base is nearly completely ossified by birth, the intraoccipital, petroccipital, and occipitomastoid sutures do not fuse until later in adulthood[6] (see **Fig. 1**).

Important Posterior Skull Base Foramina

The jugular foramen is located between the petrous portion of temporal bone (otic capsule developmentally) and the basioccipital plate and bordered anteromedially by the petroclival fissure and posterolaterally by the occipitomastoid suture. The long axis of the jugular foramen takes an oblique course running posterolateral to anteromedial. The right jugular foramen is larger than the left 68% of the time.[4]

The jugular foramen is separated from the carotid canal by the caroticojugular spine and inferomedially from the hypoglossal canal by the jugular tubercle. The intrajugular process divides the foramen into the posterolateral sigmoid and anteromedial petrosal portions of jugular foramen. Classically, the smaller anteromedial petrosal portion, also known as pars nervosa, transmits the inferior petrosal sinus and the glossopharyngeal (CN IX) nerve with its tympanic branch (Jacobson nerve). The larger posterolateral sigmoid portion, also known as pars vascularis, transmits the sigmoid sinus, forms inferiorly as the jugular

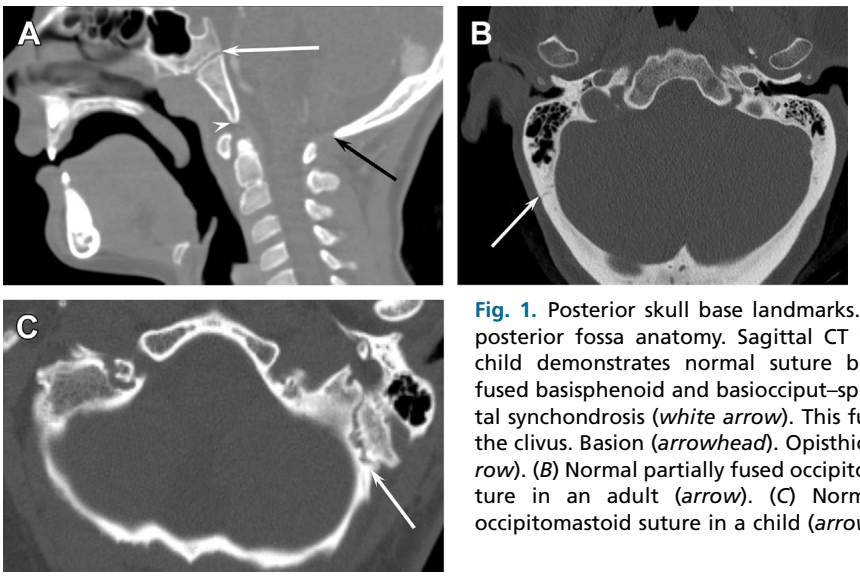

Fig. 1. Posterior skull base landmarks. (*A*) Normal posterior fossa anatomy. Sagittal CT images in a child demonstrates normal suture between unfused basisphenoid and basiocciput–spheno-occipital synchondrosis (*white arrow*). This fuses to form the clivus. Basion (*arrowhead*). Opisthion (*black arrow*). (*B*) Normal partially fused occipitomastoid suture in an adult (*arrow*). (*C*) Normal unfused occipitomastoid suture in a child (*arrow*).

bulb, and transmits the meningeal branches of the ascending pharyngeal and occipital arteries, along with the vagus (X) nerve with its auricular branch (Arnold nerve) and the accessory (XI) nerve.[6] The vagus (X) and accessory (XI) nerves, however, may travel through the pars nervosa instead of the pars vascularis.[4] The petrosal portion also receives venous tributaries from the hypoglossal canal, petroclival fissure, and vertebral venous plexus.[4]

The hypoglossal canal is located between the occipital condyle inferiorly and the jugular tubercle superolaterally.[7] The proximal portion may be divided by fibrous septa that separate the 2 roots of the hypoglossal nerve, which merge as the nerve emerges from the skull base.[8] A single hypoglossal canal occurs in 84% of cases, whereas a bipartitioned hypoglossal canal occurs in 13.5%, and a tripartitioned canal in 2.1%[9,10] (**Fig. 2**).

The foramen magnum is formed entirely within the occipital bone and is oval in shape with a longer anteroposterior dimension. The anterior margin is the basion and the posterior margin is the opisthion. Its contents include the spinal roots of the accessory nerve as they course upward from the cervical spine before heading toward the jugular bulb, the vertebral arteries, and the anterior and posterior spinal arteries.[2]

Other Posterior Skull Base Anatomic Considerations

The undersurface of the mastoid portion of the temporal bone contains the mastoid process, which is a lateral bony projection that provides attachment for the sternocleidomastoid, splenius capitis, posterior belly of digastric, and longissimus capitis muscles[8] (**Fig. 3**).

There is a groove along the medial margin of mastoid process, the mastoid notch, on which the posterior belly of the digastric muscle attaches, and posterior and medial to this is the occipital groove, which is traversed by the occipital artery (see **Fig. 3**).[8] This keeps the fairly constant relationship of the occipital artery coursing along medial margin of posterior belly of digastric muscle.

Posterior to these structures is the mastoid foramen, which is at the intersection of the temporal and occipital bones and carries mastoid emissary vein to the sigmoid sinus and a tiny branch of the occipital artery, called posterior meningeal artery traverse.[8]

There are 2 pertinent clinical scenarios to consider when these transosseous vascular channels are enlarged on a routine temporal bone CT:

- The first is an underlying abnormal high-flow vascular abnormality, such as dural arteriovenous fistula, which often has arterial supply from the occipital artery in the posterior fossa.
- The second is to notify the surgeon in a preoperative setting, to avoid inadvertent vascular injury intraoperatively.

The squamosal portion of the occipital bone contains the sagittal sulcus for the superior sagittal sinus and falx cerebri, internal occipital crest for attachment of the falx cerebelli (see **Fig. 3**), and the transverse groove for the transverse sinuses.[8] The lower surface of the basiocciput contains the

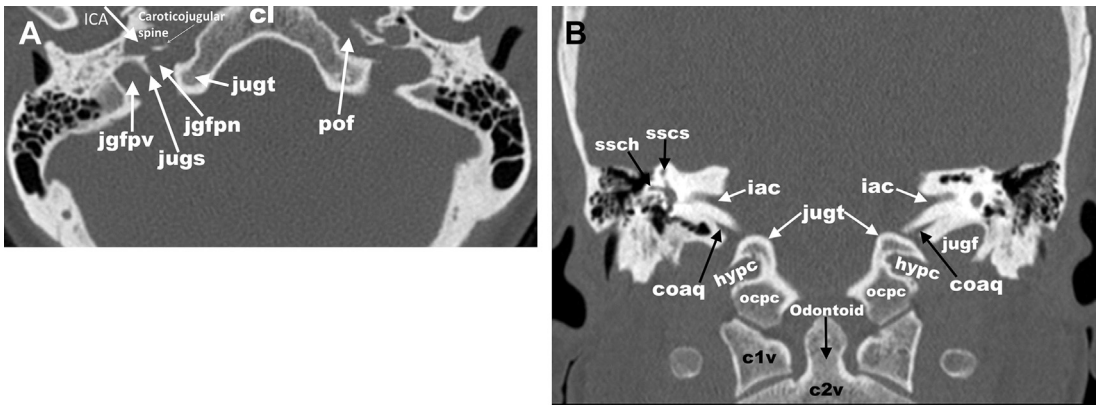

Fig. 2. Normal CT anatomy of the jugular region. Axial CT (*A*) and coronal CT (*B*) demonstrate normal bony anatomy and relationships. cl, clivus; c1v, C1 vertebra; c2v, c2 vertebra; coaq, cochlear aqueduct; hypc, hypoglossalcanal; iac, internal auditory canal; ICA, vertical segment of petrous ICA; jgfpn, pars nervosa of jugular foramen; jgfpv, pars vascularis of jugular foramen; jugf, jugular foramen; jugs, jugular spine; jugt, jugular tubercle; ocpc, occipital condyle; ssch, horizontal sumicircular canal; sscs, superior semicircular canal. (*Courtesy of* Neil Borden, MD, Pittsburgh, PA.)

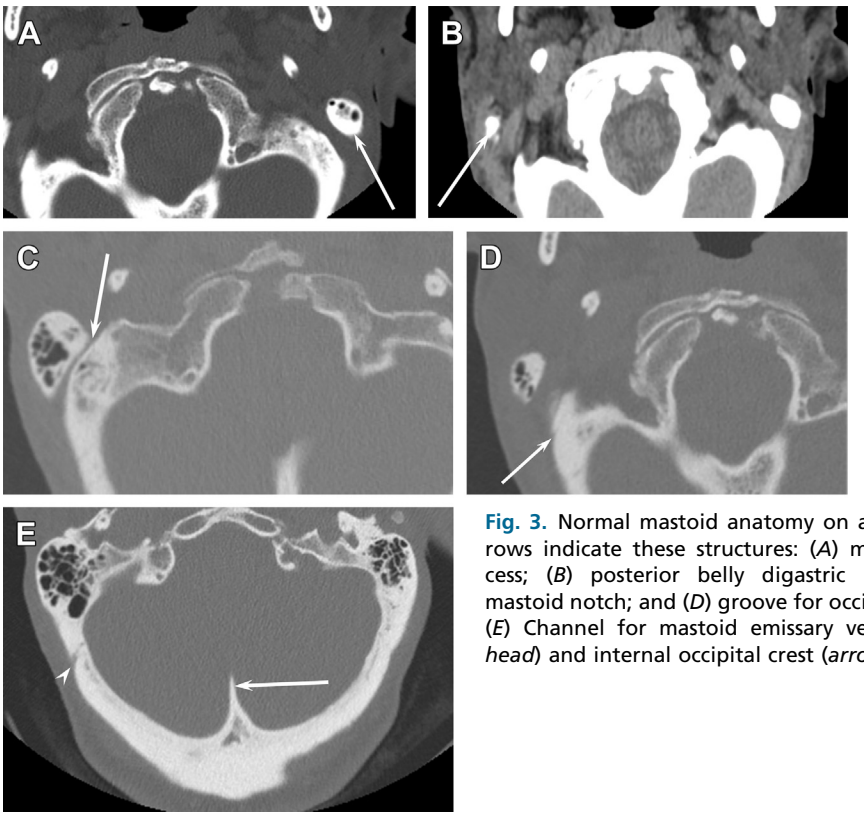

Fig. 3. Normal mastoid anatomy on axial CT. Arrows indicate these structures: (*A*) mastoid process; (*B*) posterior belly digastric muscle; (*C*) mastoid notch; and (*D*) groove for occipital artery. (*E*) Channel for mastoid emissary veins (*arrowhead*) and internal occipital crest (*arrow*).

midline pharyngeal tubercle on which the fibrous raphe of the pharynx attaches[8] (**Fig. 4**). The condylar canal and fossa just posterior to the occipital condyles receive the posterior margin of the superior facet of the atlas and an emissary vein from the transverse sinus. The upper portion of the basiocciput contains the groove for the inferior petrosal sinus[8] (see **Fig. 4**).

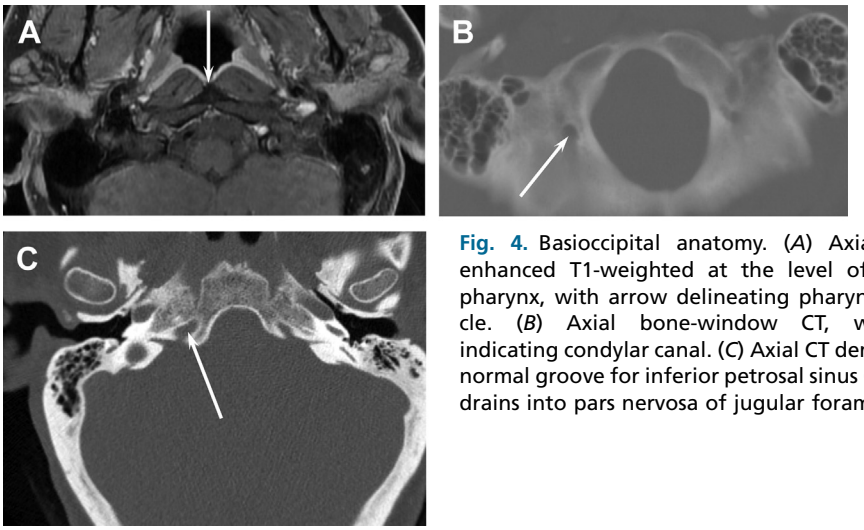

Fig. 4. Basioccipital anatomy. (*A*) Axial contrast-enhanced T1-weighted at the level of the nasopharynx, with arrow delineating pharyngeal tubercle. (*B*) Axial bone-window CT, with arrow indicating condylar canal. (*C*) Axial CT demonstrating normal groove for inferior petrosal sinus (*arrow*) as it drains into pars nervosa of jugular foramen.

SPACE-SPECIFIC SYNDROMES OF THE POSTERIOR SKULL BASE

Vernet syndrome, also known as jugular foramen syndrome, results from a constellation of CN palsies of CN IX–XI due to compression from jugular foramen lesions.[11–13]

The most common lesions involving the jugular foramen are glomus jugulare paraganglioma, schwannoma, and meningioma, of which paragangliomas makes up 80% of primary neoplasms.[6]

The classic hypervascular glomus jugulare paraganglioma, with multiple flow voids, may be multicentric in 5% to 10% of cases and even more frequently when associated with familial paraganglioma, multiple endocrine neoplasia syndrome type 1, or neurofibromatosis type 1.[14]

If there are multiple soft tissue lesions that enhance poorly on CT, neurofibromas are a consideration, and clinical history and other stigmata of neurofibromatosis should be sought for confirmation (**Fig. 5**).

Interpretation tip: If there is a lesion involving the posterior skull base, which extends into/from suprahyoid neck, it can be rapidly localized to within the carotid sheath by identifying the internal carotid artery (ICA), internal jugular vein (IJ), and styloid process. If the lesion displaces the internal carotid anteriorly and splays it apart from adjacent jugular vein, it arises from within the carotid sheath. This narrows down the primary differential considerations to paragangliomas versus nerve sheath tumors (most commonly vagal schwannomas).

Depending on the extent of the lesion, rare cases of Collet-Sicard syndrome can also develop, which is Vernet syndrome with additional CN XII palsy, or Villaret syndrome, which is Collet-Sicard syndrome with ipsilateral Horner syndrome.[15]

CRANIAL NERVE IX

The glossopharyngeal nerve is a complex mixed nerve with motor, sensory, and autonomic functions. There are 4 major nuclei in the medulla associated with CN IX functions, including[16]

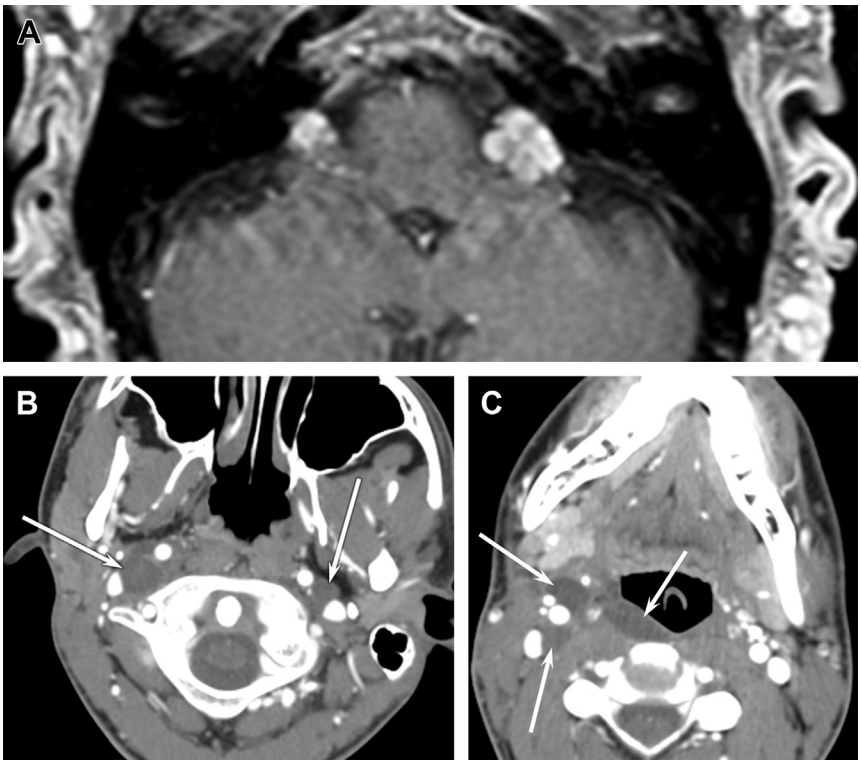

Fig. 5. Neurofibromas of the lower CNs. (*A*) Axial-enhanced T1-weighted image shows bilateral enhancing masses along the expected course of the lower CNs. (*B*) Axial-enhanced CT shows bilateral nonenhancing masses (*arrows*) at the expected location of the vagus nerves. (*C*) Axial-enhanced CT shows plexiform configuration to a nonenhancing mass (*arrows*) with involvement of the carotid and retropharyngeal spaces.

1. Nucleus ambiguous/motor nucleus: at the level of the floor of fourth ventricle, in the bulbar triangle, where special visceral efferent motor fibers arise to innervate the third pharyngeal arch and stylopharyngeus muscle
2. Inferior salivatory nucleus: responsible for general visceral efferent and parasympathetic innervation, with pathway through tympanic canaliculus
3. Solitary nucleus: responsible for special visceral afferent (taste from posterior third of tongue) at the superior aspect of nucleus and general visceral afferent (sensory receptors at the carotid body [which measures CO_2] and carotid sinus [which measures blood pressure]) at the caudal aspect of the nucleus
4. Spinal trigeminal nucleus: responsible for general somatic afferent (GSA) (sensory information of from pharynx, tongue base soft palate, and tympanic membrane)

CN IX exits from the retroolivary sulcus/postolivary sulcus and heads toward the pars nervosa of the jugular foramen.

On the routine axial plane, the cisternal segment of CN IX exits just inferior to the level of the flocculus at the level of upper medulla, where there is still a pronounced lateral contour[17] (**Fig. 6**).

The cisternal segment of CN IX is also smaller in size than its neighboring, more caudal, CN X, where the lateral contour of the medulla is more rounded.

Dysphagia and loss of sensation of posterior third of tongue (unilateral) are common symptoms with pathology affecting CN IX. Glossopharyngeal neuralgia, with symptoms of severe unilateral pharyngeal pain, is infrequent. In the setting of neurovascular compression as the cause of symptoms, the most common culprit vessel is posterior inferior cerebellar artery (PICA), followed by the vertebral artery, followed by anterior inferior cerebellar artery.[18,19]

Extracranially, CN IX's superior and inferior nuclei lie at the level of the skull base or, more precisely, in pars nervosa of the jugular foramen, where the sensory fibers of CN IX arise. Specifically, the petrosal fossula is where the more conspicuous inferior ganglion of CN IX resides and is lateral to the inferior petrosal sinus within pars nervosa.[16]

At the level of the carotid space, the nerve usually heads posterolateral to ICA in the carotid sheath, courses along the stylopharyngeus muscle (which it innervates), along pharyngeal constrictors, and across the base of tongue. It has nerve branches along the styloglossus muscle, crossing the ascending palatine artery, and innervating the inferior aspect of palatine tonsil.[16] This explains why a medialized position of styloid process has a higher likelihood of being symptomatic in Eagle syndrome, even if there is not extensive ossification of stylohyoid ligament (**Fig. 7**).

Jacobson nerve has collateral branches that communicate between CNs IX, VII, and V3.[16] It carries sensory information from the middle ear and contributes parasympathetic fibers as it courses from the superior aspect of the petrosal fossula toward the caroticojugular spine through the inferior tympanic canaliculus (**Fig. 8**) into the middle ear to the cochlear promontory, where it divides into 6 branches innervating mucosal membranes surrounding the round and oval windows, eustachian tube, and caroticotympanic nerve. These anastomose with pericarotid sympathetics and the deep greater and lesser petrosal nerves, which in turn anastomose with the superficial greater petrosal nerve to form the pterygoid nerve.[16] Also, the superficial and deep lesser petrosal nerves anastomose and head to the otic ganglion at the level of foramen ovale and the

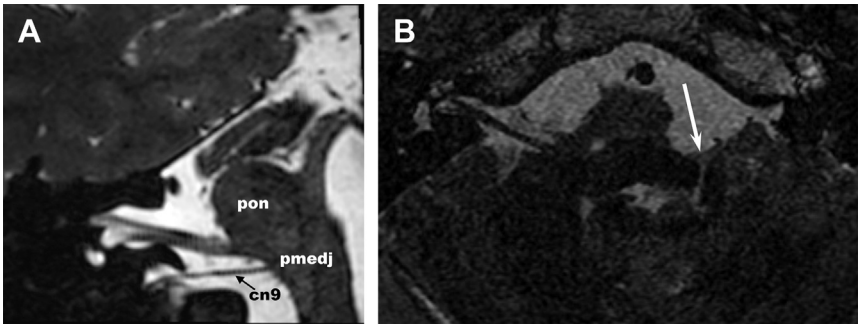

Fig. 6. Anatomy of CN IX. (*A*) Sagittal oblique SSFP sequence through the pons (pon) and pontomedullary junction (pmedj), with arrow indicating cisternal segment of CN IX (cn9). (*B*) Axial oblique SSFP image at the level of cisternal segment of left CN IX to illustrate the pronounced lateral contour of the superior medulla (*arrow*) as a useful landmark in this plane. (*Courtesy of* [*A*] Dr Neil Borden.)

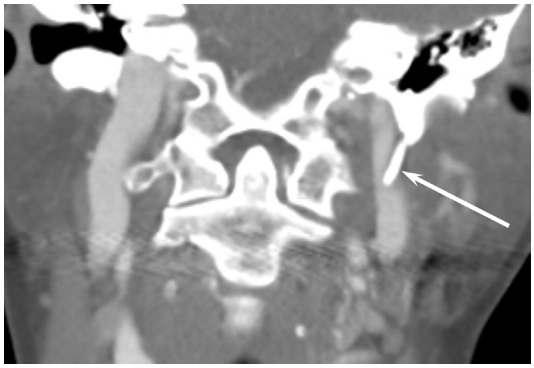

Fig. 7. Eagle syndrome. Coronal reformatted CT. A medialized styloid process (*arrow*) may cause glossopharyngeal neuralgia even without excessive ossification.

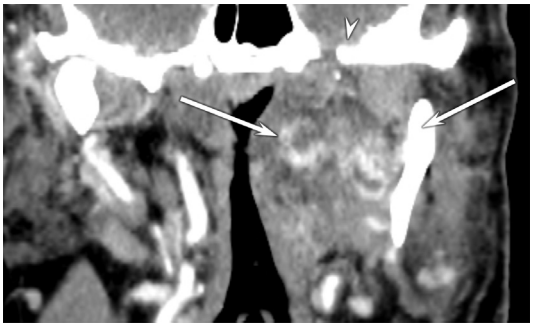

Fig. 9. Coronal CT reformat in a patient with recurrent pleomorphic adenoma demonstrates multispatial recurrent tumor (*arrows*), which involves the parotid and masticator spaces, just caudal to the level of foramen ovale (*arrowhead*) in a patient with Frey syndrome.

central skull base. From here, the otic ganglion, arises the secretory autonomic function of CN IX, which innervates the parotid gland via CN V's auriculotemporal branch.[16]

This parasympathetic pathway explains Frey syndrome, which is a potential postoperative complication from inadvertent severance and regeneration of the auriculotemporal nerve, as it innervates sweat glands in addition to parotid salivary gland, with symptoms of gustatory sweating (**Fig. 9**).

Understanding the course of Jacobson nerve is helpful when assessing the middle ear component of glomus jugulotympanicum, and glomus tympanicum tumors, as they follow branches of Jacobson nerve that form the tympanic plexus as they cross the cochlear promontory.

Glomus tumors are covered in greater detail by Jindal and colleagues (See, "Imaging Evaluation and Treatment of Vascular Lesions at the Skull Base," in this issue.).

The presence of characteristic bony hyperostosis on CT and MRI in addition to dural-based enhancement helps distinguish skull base meningioma from other pathology. Furthermore, these lesions arise from the skull base, outside the carotid sheath, and do not splay apart the IJ and ICA. If skull base meningiomas are extremely vascular, pretreatment embolization may be required prior to surgical resection.

Using bone changes to differentiate vascular lesions of the jugular bulb

- Glomus tumors cause permeative erosion.
- Schwannomas cause smooth remodeling.
- Meningiomas cause hyperostosis.

Lastly, metastases should always be considered in adults with aggressive lesions involving the skull base.

This anatomy is also key in assessing referred pain from extracranial pathology, commonly

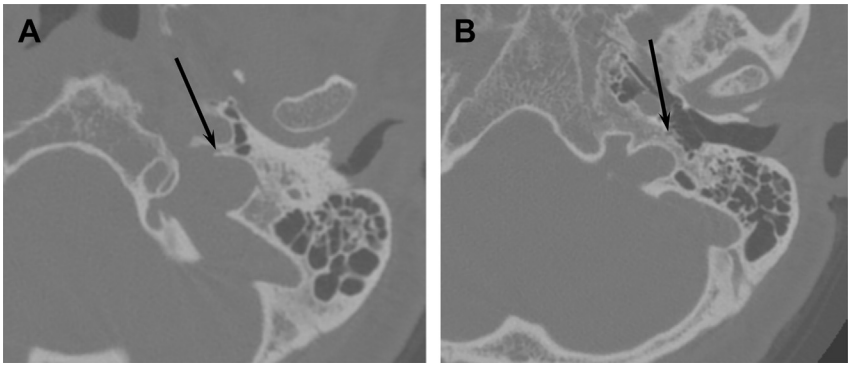

Fig. 8. Jacobson nerve. Axial CT images through the temporal bone show (*A*) inferior aspect of petrosal fossula (*arrow*) in the pars nervosa at site of the origin of Jacobson nerve as it heads toward the middle ear cavity. It is adjacent to the caroticojugular spine at this level. (*B*) Superior aspect of petrosal fossula (*arrow*) and site of origin of normal, nonenlarged inferior tympanic canaliculus, for CN IX branch–Jacobson nerve as it heads into middle ear cavity.

secondary otalgia in patients with oropharyngeal cancer as primary. Malignancies anywhere along the course of CN IX can present as otalgia and a similar principle applies to CNs V, VII, IX, and X, given considerable overlap in innervation of pharynx.[20] If no cause for otalgia is found after assessing the periauricular soft tissues, dedicated imaging of the neck should be obtained to exclude referred/secondary pain.

CRANIAL NERVE X

Function

The vagus nerve is the longest CN and is a mixed nerve, including sensory, special sensory, motor, and parasympathetic functions. It supplies sensory innervation to the middle ear, pharynx, external ear, and tympanic membrane; taste and sensation to the posterior third of the tongue in combination with CN IX; parasympathetic innervation to the aerodigestive tract; motor innervation to the laryngeal and pharyngeal constrictors and uvula; and viscerosensory innervation to the cervical, thoracic, and abdominal fibers as well as to the carotid and aortic bodies.[21]

Anatomy

With much overlap with CN IX, the intra-axial segment of the vagal nerve arises from nuclei in the medulla, dorsal to the inferior olivary nucleus, including

- Nucleus ambiguous (motor)
- Solitary tract nucleus (visceral afferents including taste)
- Dorsal or posterior motor nucleus X (visceral motor parasympathetic)
- Spinal tract and nucleus of the trigeminal nerve (sensory to the ear)

Nerve fibers exit the medulla in the postolivary sulcus to form the cisternal segment, with fibers coursing inferiorly through the medullary cistern, between CN IX and the cranial portion of CN XI (**Fig. 10**). The vagus nerve next enters the jugular foramen (its skull base segment), usually immediately posterior to the jugular spine in the pars vascularis.[2] The superior (jugular) ganglion is located in the jugular foramen, containing parasympathetic and sympathetic fibers and gives off the auricular branch of CN X.

The inferior (nodose) ganglion is located below the jugular foramen (approximately 1–2 cm).[22] Although glomus vagale tumors may arise at either the nodose ganglion or the jugular bulb, they usually tend to be centered around the nodose ganglion.[22]

The extracranial segment of CN X exits the jugular foramen into the carotid sheath, lying posterior to the internal and common carotid arteries and medial to the IJ. This relationship of the vagus nerve within the carotid sheath is helpful because mass effect from CN X pathology results in anterior displacement of ICA and lateral splaying of IJ.

In the jugular foramen, branches of CN X supply the dura of the posterior fossa (meningeal branch), external ear, and external auditory canal (auricular branch or Arnold nerve). Arnold nerve is an anastamotic branch between CN X and CN VII and arises from the superior ganglion of vagus nerve, extends into the mastoid canaliculus to anastomose with the mastoid segment of facial nerve, and extends into the tympanomastoid suture to innervate parts of tympanic membrane and skin of external

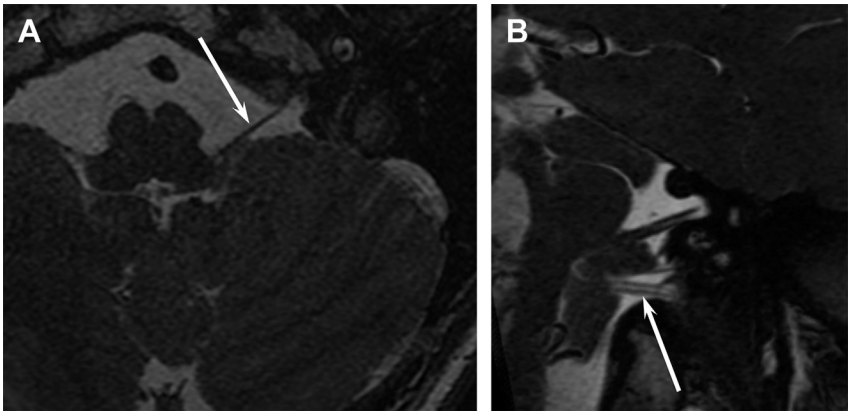

Fig. 10. Normal intracranial course of CN X. (*A*) Axial and (*B*) coronal oblique SSFP images show the vagus nerve (*arrow*), where it crosses the lateral cerebellomedullary cistern and approaches the jugular foramen. CN X is larger than CN IX (see **Fig. 7**), has 2 roots (best seen in [*B*]), and exits slightly caudal to CN IX.

auditory canal[23] (**Fig. 11**). Branches innervating the palate and pharynx, as well as branches to the carotid plexus, arise from the inferior ganglion.[24]

The superior laryngeal nerve on both sides arise just inferior to the inferior ganglion, bifurcating at the hyoid into an internal branch (which pierces the thyrohyoid membrane), carrying sensory and parasympathetic innervation to the larynx, and the external branch, carrying motor to the cricothyroid and inferior pharyngeal constrictor. Similar to the glossopharyngeal nerve, this accounts for referred pain from pharyngeal pathology presenting as otalgia. Inferior to the superior laryngeal nerve, the superior and inferior branches of the cardiac nerve arise, communicating with sympathetic fibers.[23]

The inferior (or recurrent) laryngeal nerve arises near the thoracic inlet on both sides. On the right, it loops behind the subclavian artery, coursing superiorly in the tracheoesophageal groove. On the left, it loops under the aortic arch, posterior to the ligamentum arteriosum, and then follows a similar course. On both sides, it passes under the posterior suspensory ligament extending from the cricoid to the first tracheal rings, entering the larynx at the level of the cricoarytenoid joint. The recurrent laryngeal nerve supplies all of the intrinsic laryngeal musculature, except the cricothyroid muscle.[4]

The vagus nerve also innervates the cardiac plexus, pulmonary plexus, esophagus, stomach, celiac plexus, solid organs, and intestines.[4]

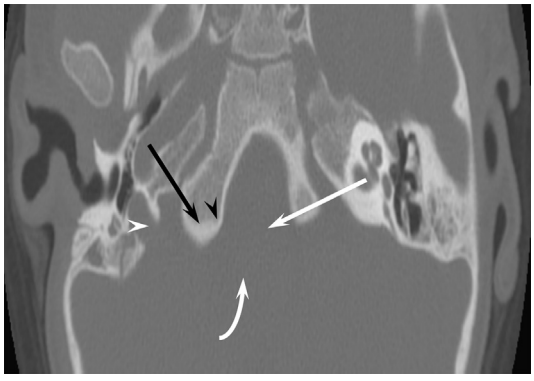

Fig. 11. Arnold nerve. Axial CT with several adjoining anatomic structures labeled. White arrow, minor contour irregularity along pars vascularis of jugular foramen at the expected site of mastoid canaliculus; white arrowhead, tympanomastoid suture along posterior wall of external auditory canal, carrying Arnold nerve; black arrowhead, vertical/mastoid segment of facial nerve canal; curved arrow, anterior portion of occipitomastoid suture (unfused because the patient is a child); black arrow, chorda tympani.

Pathology and Localization

If the vagus nerve is involved in association with CN IX, XI or XII, imaging should focus on the medulla, premedullary cistern, and jugular foramen, where a single lesion can easily involve multiple nerves.

Infarct of the lateral medulla (usually PICA occlusion) is known to cause lateral medullary, or Wallenberg, syndrome. In addition to the classic loss of pain and temperature sensation on the contralateral body and ipsilateral face, there is ipsilateral pharyngeal and palatal hemiparalysis, decreased pharyngeal gag reflex, and ipsilateral vocal cord paralysis due to involvement of the vagal nerve nuclei. These clinical findings, along with vertigo, help differentiate Wallenberg syndrome from lateral pontine syndrome, usually caused by anterior inferior cerebellar artery occlusion (**Fig. 12**).

Lesions that extend into cerebellomedullary cistern include meningiomas, schwannomas, arachnoid cysts, and epidermoid tumors and can involve CN X in addition to neighboring lower CNs. If large enough, they may extent into the cerebellopontine cistern with mass effect on CNs VII and VIII (**Fig. 13**).

In addition to multiple lower CN neuropathies, lesions at the level of the jugular foramen/skull base may present as a painless submucosal neck mass or as symptoms secondary to eustachian tube dysfunction from local mass effect.

The 2 most common tumors in the carotid sheath below the skull base are schwannomas and glomus vagale tumors. Suprahyoid vagal schwannomas are the most common carotid space schwannomas and, unlike glomus vagale tumors, gross total resection can occasionally be achieved without sacrificing the nerve. Larger lesions may have intratumoral nonenhancing regions (**Fig. 14**). Vagal schwannomas can be

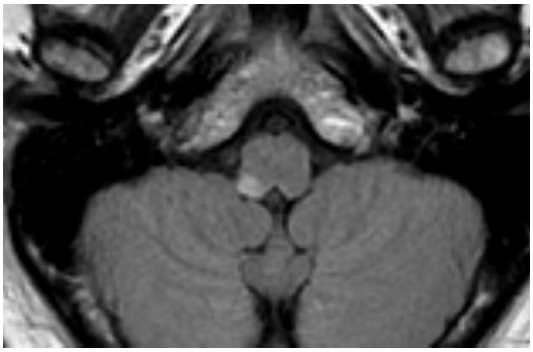

Fig. 12. Lateral medullary syndrome. FLAIR image demonstrates acute infarct involving the right dorsal-lateral medulla.

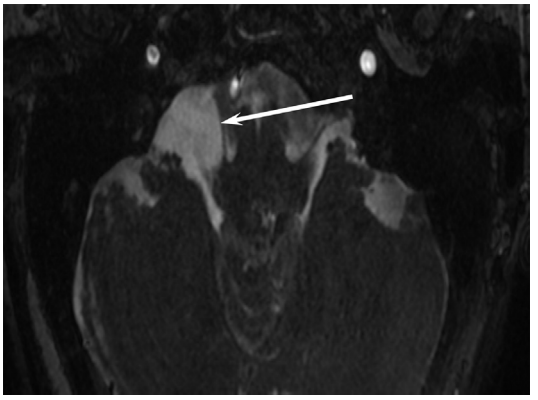

Fig. 13. Axial SSFP image demonstrates an arachnoid cyst in the lateral medullary cistern causing medial and ventral displacement of lower CNs IX and X (*arrow*).

distinguished from other pathology in this region by

- Localizing pathology to the carotid sheath in the suprahyoid neck by noticing anterior displacement of the ICA and splaying from the IJ. Specifically, other pathology in the suprahyoid neck, including sympathetic chain schwannoma (which is medial to and will not splay apart ICA and IJ as it is along the medial margin of carotid sheath), and pathology arising from masticator space, parotid space, and prestyloid parapharyngeal space will not anteriorly displace ICA or splay apart ICA and IJ.
- Superomedial course of lesion toward brainstem
- Smooth osseous margins on CT (**Fig. 15**)
- Heterogeneous enhancement on MR, without large flow voids

Paralysis of the constrictor muscles of the pharynx as well as vocal cord paralysis supports a cause of vagal neuropathy proximal/cranial to the origin of the recurrent laryngeal nerve. The findings of ipsilateral oropharyngeal dilation and thinning of the pharyngeal constrictors, as well as contralateral uvular deviation, support involvement at the level of the pharyngeal plexus origin[25] and should prompt investigation with MRI of the brainstem and skull base.

Isolated vocal cord paralysis (without other findings of CN X pathology) places the level of the pathology below the hyoid.[17] An ipsilateral thyroid mass associated with unilateral vocal cord palsy is considered a worrisome feature by imaging and warrants follow-up and tissue sampling of dominant thyroid nodule.[26,27]

Imaging Protocol for Hoarseness

When there is a known laryngeal primary, CT neck should be centered at the level of true vocal cords, with thin cuts and reconstructions to optimally characterize extent of local and regional disease. Split bolusing of contrast may be considered to optimize characterization of mucosal lesions.

When there is vocal cord paralysis as a presenting symptom, with unknown pathology, caudal extent of imaging field of view should cover the subclavian artery if the right side is symptomatic and should cover the aortopulmonary window if the left is symptomatic, with imaging acquired during quiet respiration.

CRANIAL NERVE XI

CN XI is a pure motor nerve, innervating the trapezius and sternocleidomastoid muscles. Gray's *Anatomy of the Human Body*[28] and other historical texts describe a "Cranial part" and a "Spinal part" to the nerve. The cranial part arises from the nucleus ambiguus and exits into the postolivary sulcus, just below the vagus nerve. This component joins the vagus nerve at the inferior ganglion, becoming inseparable from the vagus more inferiorly. Most

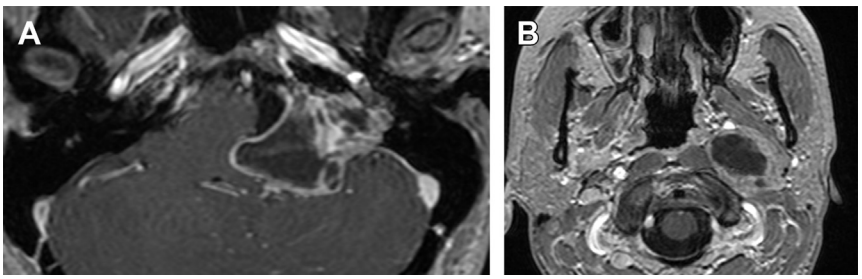

Fig. 14. Vagus schwannoma. Postcontrast axial MRI in the (*A*) lateral medullary cistern and (*B*) upper neck demonstrate a heterogeneously enhancing mass with imaging characteristics similar to a vestibular schwannoma, but a more inferior location and involvement of the jugular bulb. (*B*) Extension into the carotid sheath is common for lesions that arise in the jugular bulb.

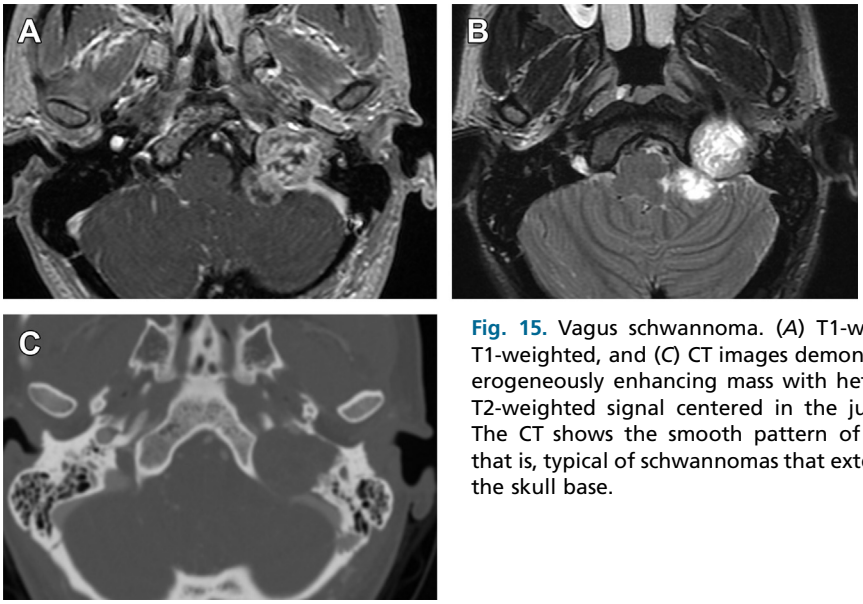

Fig. 15. Vagus schwannoma. (*A*) T1-weighted, (*B*) T1-weighted, and (*C*) CT images demonstrate a heterogeneously enhancing mass with heterogeneous T2-weighted signal centered in the jugular fossa. The CT shows the smooth pattern of remodeling that is, typical of schwannomas that extend through the skull base.

modern investigators consider this cranial part and medial branch a component of the vagus nerve and the spinal part alone to be CN XI.[29–40]

The spinal part arises from motor fibers of the spinal nucleus, which extends from C1 to C5 as a column of cells posterior to the anterior horn called the spinal accessory nucleus. Fibers arise from the lateral margin of the cervical cord, between the anterior and posterior spine rootlets, and run superiorly through foramen magnum, laterally over the condyle into the pars vascularis of the jugular foramen.

The spinal accessory nerve exits the jugular foramen with the vagus nerve and the posterior meningeal artery into the carotid space. It courses along inferior border of the digastric muscle to reach the deep margin of sternocleidomastoid muscle approximately 4 cm below the mastoid bone. After receiving anastomotic branches from cervical C3 to C5 nerves, it terminates along the undersurface of the trapezius muscle.

The most common cause of isolated CN XI palsy is injury during a surgical neck dissection and presents clinically as inability to shrug the shoulder. Radiographically, it can be appreciated as atrophy of the sternocleidomastoid and trapezius and, eventually, compensatory hypertrophy of the levator scapulae, which should not be mistake for a neck mass (**Fig. 16**).

Imaging for potential cause of CN XI palsy when associated with other lower CN palsies should focus on the brainstem and jugular foramen as well as the craniocervical junction (**Fig. 17**).

CRANIAL NERVE XII

The hypoglossal nerve has a purely motor function, innervating intrinsic and a majority of the extrinsic tongue musculature (the exception being the palatoglossus muscle, which is innervated by the vagus nerve).

The hypoglossal nerve can be divided into 5 segments: medullary, cisternal, skull base, carotid space, and sublingual.

The medullary segment of the hypoglossal nerve originates from the hypoglossal nucleus within the medulla and extends through the medulla

Fig. 16. CN XI palsy. The sternocleidomastoid muscle (*white arrow*) and the trapezius muscle (*black arrow*) are atrophied, whereas the levator scapulae muscle (*arrowhead*) is hypertrophied to compensate.

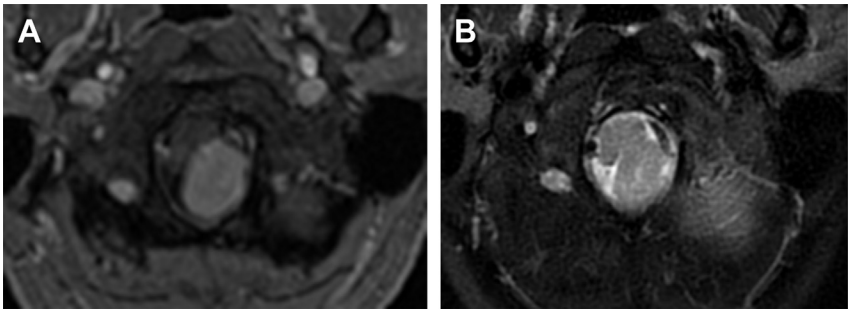

Fig. 17. Schwannoma of CN XI. Axial (*A*) T1-weighted and (*B*) T2-weighted images show a uniformly enhancing lesion arising in the posterolateral foramen magnum with T2-weighted signal isointense to the brainstem. The tumor forms sharp angles with underlying bone, unlike the more common meningioma.

oblongata in a paramedian location. The nerve fibers (approximately 10–12) have the most anterior point of exit from the medulla relative to the other lower CNs, in the preolivary sulcus, posterolateral to the vertebral artery. The vertebral arteries then course caudal to the inferior most nerve roots within the premedullary cistern, before CN XII exits the posterior skull base via the hypoglossal canal (Fig. 18). Emerging from the hypoglossal canal, the hypoglossal nerve enters the carotid space where it courses inferiorly and passes between the ICA and IJ, superficial to the vagus nerve, to the level of the angle of the mandible, making a large curve. Near the level of the carotid bifurcation, the nerve loops anteriorly around the root of the occipital artery, inferior to the posterior belly of the digastric muscle. At the level of the hyoid bone, the nerve crosses the lingual artery and curves anteriorly along the surface of the hyoglossus muscle, lateral to the lingual artery within the sublingual space. As it travels further anteriorly, the hypoglossal nerve lies on the surface and pierces the genioglossus muscle (Fig. 19).

The cervical portions of the nerve expose it to injury during neck surgeries, despite its lack of primary innervation in the neck.

During its course, it gives off multiple branches, notably meningeal branch, anastomotic branches with the superior cervical sympathetic ganglion, cervical plexus, and inferior ganglion of vagus nerve. Anastamoses with C1–C3 and CN XII descending branch form ansa cervalis and there are minor branches, which communicate with V3 and the lingual nerve.[16]

Damage to the hypoglossal nerve is uncommon as an isolated CN palsy. Possible causes include tumors and penetrating traumatic injury. If the clinical symptoms are accompanied by acute pain, a possible cause may be dissection of the ICA (Fig. 20).

Although the tongue usually atrophies on the side ipsilateral to the lesion, supranuclear disease affecting CN XII results in paralysis of the tongue contralateral to the side of the lesion. Deviation of the tongue occurs away from the side of the lesion in supranuclear pathology.

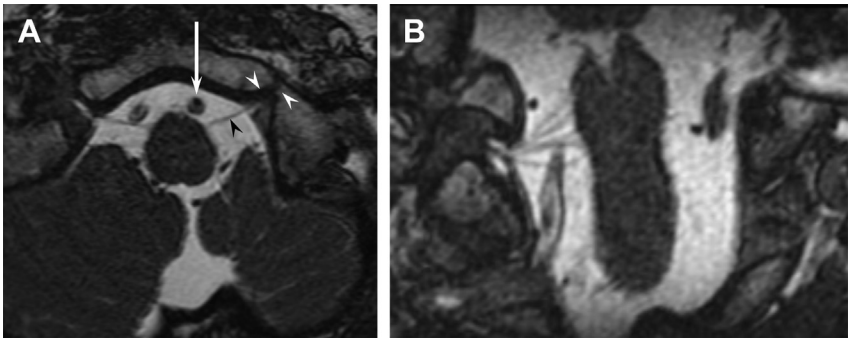

Fig. 18. Cisternal course of hypoglossal nerve. (*A*) Axial SSFP MRI shows the oblique course of the hypoglossal nerve (*black arrowhead*) as it crosses the lateral cerebellomedullary cistern toward the hypoglossal canal (*white arrowheads*). The vertebral artery (*arrow*) is anterior to the nerve. (*B*) Coronal SSFP image reveals the numerous nerve rootlets that compose right CN XII.

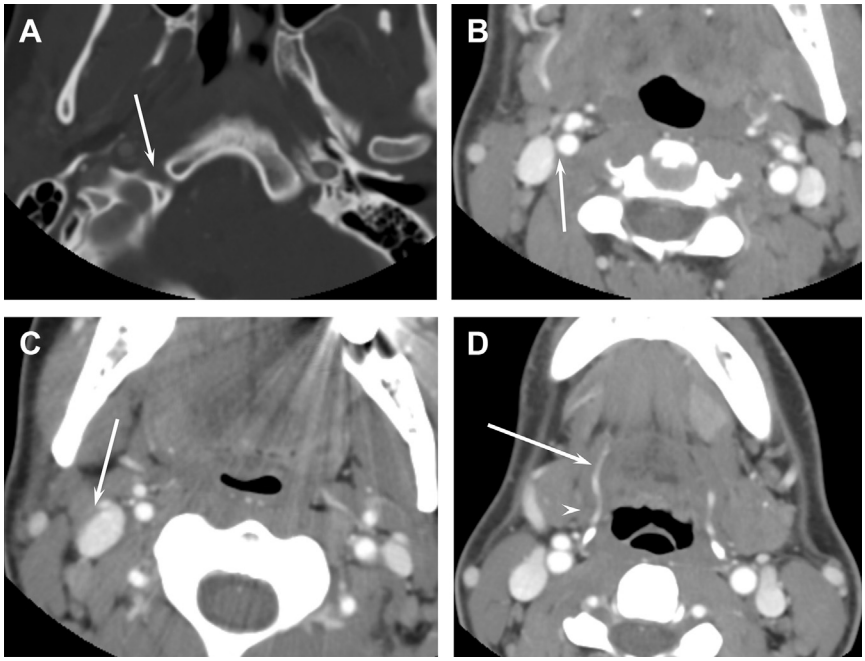

Fig. 19. Cervical course of hypoglossal nerve. Axial CT images with arrows showing the expected course of CN XII through (*A*) hypoglossal canal; (*B*) carotid space posterior to the vessels; and (*C*) medial aspect of posterior belly of digastric muscles, along with the occipital artery and (*D*) crossing the lingual artery and curving anteriorly along the surface of the hyoglossus muscle (*arrowhead*), lateral to the lingual artery within the sublingual space.

Fasciculation and tongue atrophy are absent in these cases.

When pathology affects the hypoglossal nerve at the nuclear or infranuclear level, the clinical symptoms are ipsilateral. Patients present with deviation of the tongue toward the damaged side when asked to stick out their tongue as well as possible muscle wasting and twitching of muscle fibers on the affected side, with longstanding imaging findings including fatty atrophy (**Fig. 21**).

Imaging pearl: If fatty hemiatrophy of tongue is noted on a neck CT, carefully scrutinize the posterior skull base and hypoglossal canal to exclude underlying pathology that would account for denervation of CN XII. Dedicated imaging of the brain should be considered if no cause is identified.

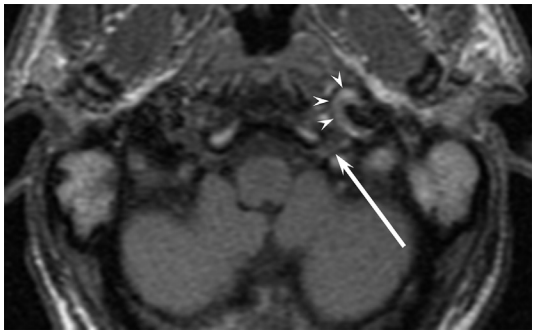

Fig. 20. Vertebral artery dissection causing hypoglossal paralysis. T1-weighted noncontrast image demonstrates crescentic region of intrinsic T1-weighted shortening (*arrowheads*) surrounding a high cervical ICA, indicating dissection. Notice its proximity to the hypoglossal nerve and canal (*arrow*).

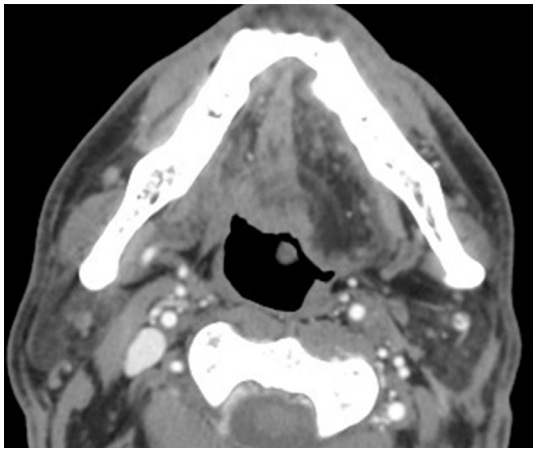

Fig. 21. Fatty atrophy of the tongue from hypoglossal denervation. CT demonstrates asymmetry of density within the tongue, with a sharp midline demarcation. The left side of the tongue musculature has atrophied from injury to CN XII.

Pathologies that involve the skull base segment of CN XII include meningiomas (**Fig. 22**); primary nerve sheath tumors; metastases; local extension of tumors, such as nasopharyngeal carcinoma, glomus tumors, or lymphoma (**Fig. 23**); and aggressive skull base infection (**Fig. 24**).

VARIANT ANATOMY AND PATHOLOGY

Bony Variants

Chamberlain line (**Fig. 25**) and Welcher basal angle (**Fig. 26**) can help quickly identify the presence of bony anomalies involving the posterior skull base and craniocervical junction.

Most anomalies of the occiput are associated with platybasia (Welcher basal angle greater 140°) and basilar invagination (cranial extension of dens and anterior arch of C1 above Chamberlain line in the setting of normal bone). These findings should prompt a search for other posterior skull base abnormalities, such as complete or partial occipital assimilation of the atlas, basioccipital hypoplasia, or condylar dysplasia.[41]

Chiari I malformations, defined as descent of the cerebellar tonsils 5 mm or more below the foramen magnum on imaging (**Fig. 27**), are also frequently associated with basilar invagination. Normal position of the cerebellar tonsils does demonstrate minor variation with age with the lowest point somewhere between 5 and 15 years of age.[42,43] Symptomatic patients demonstrate not only inferior descent of the cerebellar tonsils but also a typically a compression of the brainstem, cerebellar tonsils (which lose their normal rounded configuration and become peg like), foramen of Magendie and foramen of Luschka, and central canal of the cord (causing hydrosyringomyelia and cranial neuropathies).[44–46]

Cerebrospinal fluid flow studies may be useful to assess flow surrounding the cervicomedullary junction[47] and help in selecting appropriate candidates for decompressive surgery, which include suboccipital craniectomy with or without C1/C2 laminectomy, with or without duroplasty, opening of the arachnoidal membrane, lysis of intradural adhesions, partial tonsillar resection, plugging of the obex, leaving the dura open, and/or posterior fossa reconstruction with cranioplasty.[48–51]

The variations of the arteries and veins are covered by Jindal and colleagues (See, "Imaging

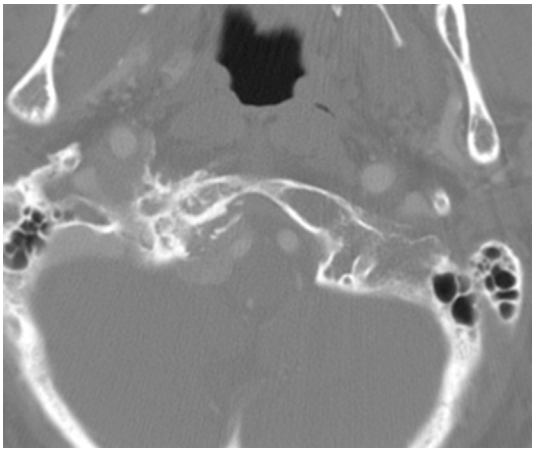

Fig. 22. Meningioma causing hypoglossal denervation. Axial-enhanced CT shows a mass surrounding the hypoglossal canal with the characteristic hyperostosis of a meningioma.

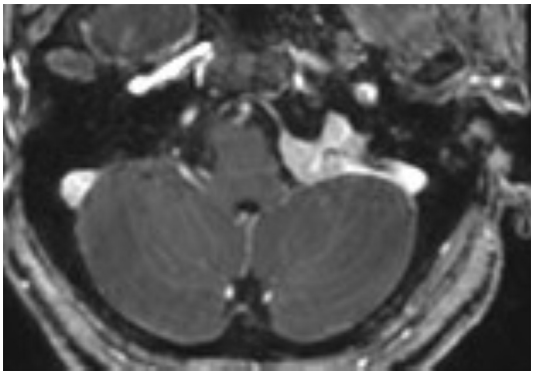

Fig. 23. Lymphoma causing hypoglossal denervation. Axial-enhanced T1-weighted image shows a broad-based dural lesion overlying and extending into the left hypoglossal canal. This could be easily mistaken for a meningioma.

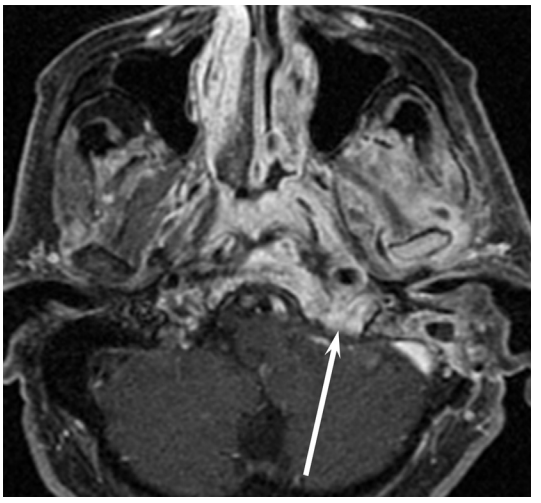

Fig. 24. Skull base osteomyelitis causing hypoglossal denervation. Axial-enhanced T1-weighted image shows extensive enhancement of the left skull base and surrounding tissues, in particular the hypoglossal canal (*arrow*).

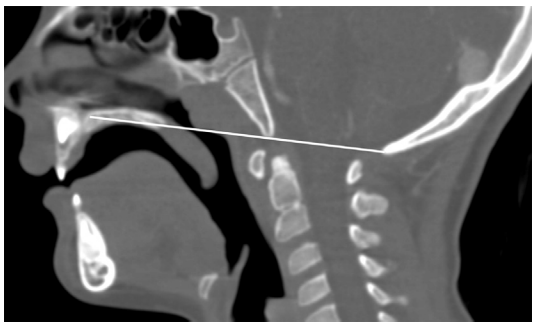

Fig. 25. Chamberlain line. This line is drawn from the hard palate to the opisthion. If the dens extends above this line, the patient has basilar invagination.

Evaluation and Treatment of Vascular Lesions at the Skull Base," in this issue.).

BONE TUMORS

Chordomas and chondrosarcomas are the most common primary bone tumors of the skull base, and there is much overlap in their clinical presentation, imaging characteristics, and management.[52–67] Both are hyperintense on T2-weighted sequences, and both are treated with wide local excision. MRI and CT play complementary roles in arriving at an accurate diagnosis.

Langerhans cell histiocytosis, although most frequently seen in children, can be seen at any age and is considered benign. Although calvarial Langerhans cell histiocytosis is most common, the preferred site of skull base involvement is the temporal bones followed by the sphenoid bone. CT is helpful in evaluation and differentiating from other pathology, by showing lack of matrix or fat within the lesion (**Fig. 28**). On MRI, although there is usually a fairly focal lesion on T1-weighted and T2-weighted sequences, associated peripheral enhancement beyond the margins of the lesion usually prompts tissue sampling to exclude a more aggressive process.

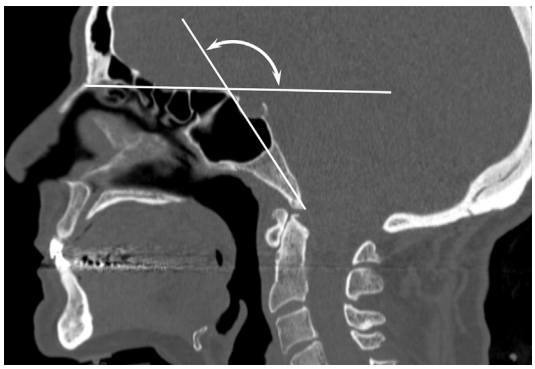

Fig. 26. Welcher basal angle. Lines are drawn between the nasion and tuberculum sella and between the basion and tuberculum sella. If the resulting angle is greater than 140°, the patient has platybasia.

Fig. 27. Chiari I malformation. Sagittal T1-weighted image shows a black line along the foramen magnum and a black arrow depicting the severe herniation of cerebellar tonsils below the foramen magnum. Because the arrow is longer than 5 mm, and there is no posterior fossa mass or mass effect, this patient has a Chiari malformation. Note the associated basilar invagination, with the anterior arch of C1 and dens extending superior to Chamberlain line (*white line*).

Giant cell tumors, primarily occurring in the epiphyses of long bones, are rare in the skull base. Giant cell tumors are derived from differentiated mesenchymal cells of the bone marrow and should be differentiated from giant cell reparative granulomas, which are reactive bone lesions most frequently occurring in the mandible and maxilla.[68–70]

Plasmacytoma is a separate entity from multiple myeloma in that it is localized to a single site and can occur anywhere in the skull base. CT findings include an expansile, lytic slightly hyperdense lesion involving the diploic space as well as the inner and outer tables of calvarium with mass effect on the adjacent brain parenchyma. MRI characteristics of solitary plasmacytoma include T1-weighted signal isointensity and isointense or slightly hyperintense signal on T2-weighted images, with homogeneous enhancement after administration of intravenous gadolinium.[71–77]

DIFFUSE BONE ABNORMALITIES

Diffuse bony abnormalities may be secondary to metabolic disorders; chronic severe anemia from hemoglobinopathies, such as sickle cell disease; or malignancy, such as multiple myeloma.

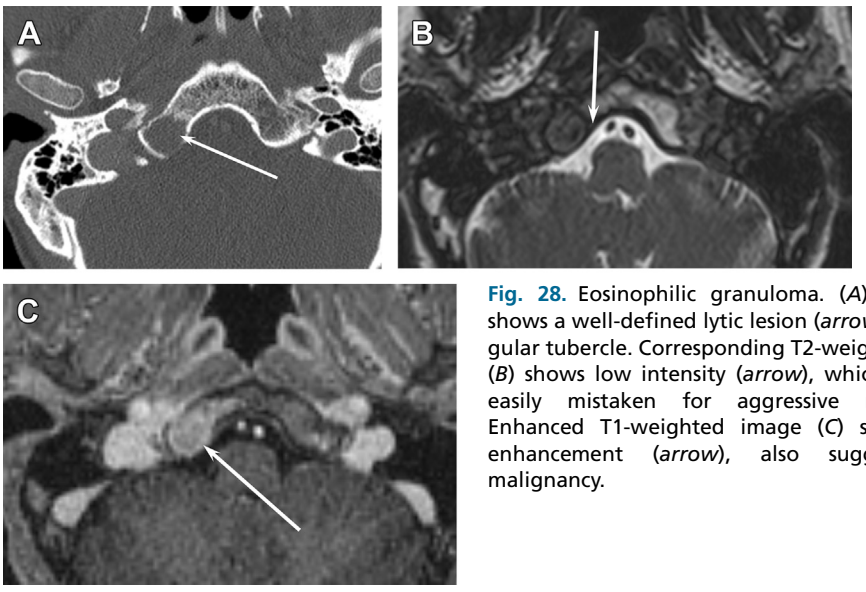

Fig. 28. Eosinophilic granuloma. (*A*) CT image shows a well-defined lytic lesion (*arrow*) in the jugular tubercle. Corresponding T2-weighted image (*B*) shows low intensity (*arrow*), which could be easily mistaken for aggressive malignancy. Enhanced T1-weighted image (*C*) shows brisk enhancement (*arrow*), also suggestive of malignancy.

The primary differential considerations for geographic areas of bony abnormality are fibrous dysplasia and Paget disease, which are discussed elsewhere in this issue (See C. Douglas Phillips and Lindsey M. Conleys' article, "Imaging of the Central Skull Base," in this issue.).

TRAUMA

There are 3 types of occipital condylar fractures:

Type1 is a comminuted fracture of occipital bone with preservation of alar ligament and tectorial membrane (**Fig. 29**).

Type 2 is a fracture plane extending anteriorly to involve the occipital condyle and basiocciput. The alar ligament and tectorial membrane, however, are intact by imaging.

Type 3 is disruption of the alar ligament and tectorial membrane.

Coronal is the best plane to quickly find a small avulsion fracture off the occipital condyle (**Fig. 30**).

Clival fractures suggest a high-energy mechanism, with frequent with injury to the brainstem and posterior arterial circulation. CTA may be considered to better assess for associated vascular injury.[16]

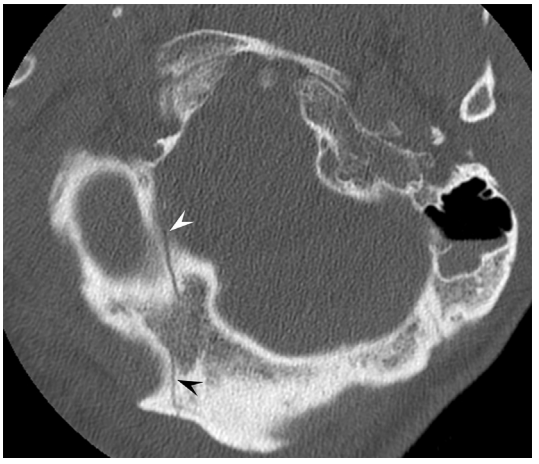

Fig. 29. Type 1 occipital bone fracture. Axial CT demonstrates a fracture line (*arrowheads*) through the lateral aspect of the condyle, where it does not affect the alar ligament or tectorial membrane.

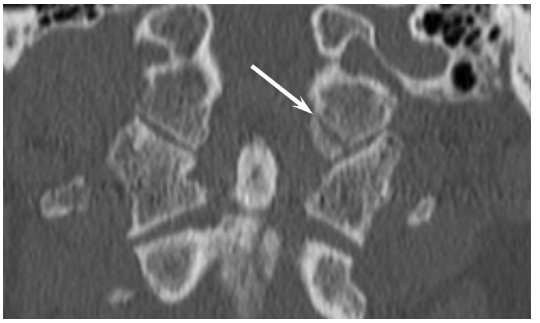

Fig. 30. Occipital avulsion. Coronal reformatted CT shows a fracture plane through the occipital condyle (*arrow*) into the atlanto-occipital junction. This is usually accompanied by an injury to the alar ligament (type 3 occipital bone fracture).

A persistent Kerckring ossicle is a small ossicle at the posterior margin of the foramen magnum, which is normally unfused in 50% of term newborns and usually fuses with the supraoccipital suture by 1 year.[3] It should not be mistaken for an avulsion fracture in this demographic.

REFERENCES

1. Kent DT, Rath TJ, Snyderman CH. Conventional and 3-dimensional computerized tomography in Eagle's syndrome, glossopharyngeal neuralgia, and asymptomatic controls. Otolaryngol Head Neck Surg 2015; 153(1):41–7.
2. Morani AC, Ramani NS, Wesolowski JR. Skull base, orbits, temporal bone, and cranial nerves: anatomy on MR imaging. Magn Reson Imaging Clin N Am 2011;19:439–56.
3. Harnsberger HR, Macdonald AJ. Diagnostic and surgical imaging anatomy. Brain, head & neck, spine. Salt Lake City (UT): Amirsys; 2006.
4. Rhoton AL Jr. Jugular foramen. Neurosurgery 2000; 47(Suppl 3):S267–85.
5. Rhoton AL Jr, Buza R. Microsurgical anatomy of the jugular foramen. J Neurosurg 1975;42:541–50.
6. Ong CK, Fook-Hin Chong V. Imaging of jugular foramen. Neuroimaging Clin N Am 2009;19:469–82.
7. Voyvodic F, Whyte A, Slavotinek J. The hypoglossal canal: normal MR enhancement pattern. AJNR Am J Neuroradiol 1995;16:1707–10.
8. Gray H, Warwick R, Williams PL. Gray's anatomy. Philadelphia: Saunders;Churchill Livingstone; 1980.
9. Murlimanju BV, Chettiar GK, Krishnamurthy A, et al. The paracondylar skull base: anatomical variants and their clinical implications. Turk Neurosurg 2015;25:844–9.
10. Drake RL, Vogl W, Mitchell AWM. Gray's basic anatomy. Edinburgh (United Kingdom): Churchill Livingstone; 2012.
11. Jo YR, Chung CW, Lee JS, et al. Vernet syndrome by varicella-zoster virus. Ann Rehabil Med 2013;37: 449–52.
12. Jackson CG. Glomus tympanicum and glomus jugulare tumors. Otolaryngol Clin North Am 2001;34: 941–70, vii.
13. Robertson JH, Gardner G, Cocke EW Jr. Glomus jugulare tumors. Clin Neurosurg 1994;41:39–61.
14. Wharton SM, Davis A. Familial paraganglioma. J Laryngol Otol 1996;110:688–90.
15. Lustrin ES, Palestro C, Vaheesan K. Radiographic evaluation and assessment of paragangliomas. Otolaryngol Clin North Am 2001;34:881–906, vi.
16. Leblanc A. Anatomy and imaging of the cranial nerves. London: Springer; 1991.
17. Mukherji S. Cranial Nerves. Neuroimaging Clin N Am 2008;18(2):xiii.
18. Hiwatashi A, Matsushima T, Yoshiura T, et al. MRI of glossopharyngeal neuralgia caused by neurovascular compression. AJR Am J Roentgenol 2008;191(2): 578–81.
19. Weissman J, Hirsch B. Beyond the promontory: the multifocal origin of glomus Tympanicum Tumors. AJNR Am J Neuroradiol 1998;19:119–22.
20. Chen RC, Khorsandi AS, Shatzkes DR, et al. The radiology of referred otalgia. AJNR Am J Neuroradiol 2009;30(10):1817–23.
21. Osborn A. Osborn's brain: imaging, pathology, and anatomy. Salt Lake City (Utah): Amirsys; 2013. p. 623–4.
22. Weissman JL. Case 21 Glomus vagale tumor. Radiology 2000;215(1):237–42.
23. Netter FH. Atlas of human anatomy. 5th edition. Philadelphia: Saunders/Elsevier; 2011. Plate 120.
24. Rubinstein D, Burton BS, Walker AL. The anatomy of the inferior petrosal sinus, glossopharyngeal nerve, vagus nerve, and accessory nervein the jugular foramen. AJNR Am J Neuroradiol 1995;16: 185–94.
25. Sreevasta MR, Srinivasarao RV. Three cases of vagal nerve shwannoma and review of the literature. Indian J Otolaryngol Head Neck Surg 2011;63(4): 310–2.
26. Abboud B, Tabchy B, Jambart S, et al. Benign disease of the thyroid gland and vocal fold paralysis. J Laryngol Otol 1999;113(5):473–4.
27. Paquette C, Manos D, Psooy BJ. Unilateral vocal cord paralysis: a review of CT findings, mediastinal causes, and the course of the recurrent laryngeal nerves. RadioGraphics 2012;32(3):721–40.
28. Gray H. Anatomy of the human body. Philadelphia: Lea & Febiger; 1918. Bartleby.com, 2000.
29. Ryan S, Blyth P, Duggan N, et al. Is the cranial accessory nerve really a portion of the accessory nerve? Anatomy of the cranial nerves in the jugular foramen. Anat Sci Int 2007;82:1–7.
30. Thompson EO, Smoker WRK. Hypoglossal nerve palsy: a segmental approach. Radiographics 1994; 14:939–58.
31. Smoker WRK. The hypoglossal nerve. Neuroimaging Clin N Am 1993;3:193–207.
32. Macedo TF, Gow PJ, Heap SW, et al. Bilateral hypoglossal nerve palsy due to vertical subluxation of the odontoid process in rheumatoid arthritis. Br J Rheumatol 1988;27:317–20.
33. Fujita N, Shimada N, Takimoto H, et al. MR appearance of the persistent hypoglossal artery. AJNR Am J Neuroradiol 1995;16:990–2.
34. Goldstein JH, Woodcock H, Phillips D. Complete duplication or extreme fenestration of the basilar artery. AJNR Am J Neuroradiol 1999;20:149–50.
35. Kodama N, Ohara H, Suzuki J. Persistent hypoglossal artery associated with aneurysms. Report of two cases. J Neurosurg 1976;45:449–51.
36. Kobanawa S, Atsuchi M, Tanaka J, et al. Jugular bulb diverticulum associated with lower cranial

nerve palsy and multiple aneurysms. Surg Neurol 2000;53:559–62.
37. Overton SB, Ritter FN. A high placed jugular bulb in the middle ear: a clinical and temporal bone study. Laryngoscope 1973;83:1986–91.
38. Weiss RL, Zahtz G, Goldofsky E, et al. High jugular bulb and conductive hearing loss. Laryngoscope 1997;107:321–7.
39. Lee M, Kim M. Image findings in bran developmental venous anomalies. J Cerebrovasc Endovasc Neurosurg 2012;14(1):37–43.
40. Alatakis S, Koulouris G, Stuckey S. CT-Demonstrated transcalvarial channels diagnostic of dural arteriovenous fistula. AJNR Am J Neuroradiol 2005; 26:2393–6.
41. Smoker W. Craniovertebral junction: normal anatomy, craniometry and congenital anomalies. Radiographics 1994;14(2):255–77.
42. Speer MC, Enterline DS, Mehltretter L, et al. Review article: chiari type i malformation with or without syringomyelia: prevalence and genetics. J Genet Couns 2003;12:297–311.
43. Kornienko VN, Pronin IN, editors. Diagnostic neuroradiology. 1st edition. Berlin: Springer Berlin; 2008. 1 online resource.
44. Sarnat HB. Disorders of segmentation of the neural tube: Chiari malformations. Handb Clin Neurol 2008;87:89–103.
45. Schijman E. History, anatomic forms, and pathogenesis of Chiari I malformations. Childs Nerv Syst 2004;20:323–8.
46. Goh S, Bottrell CL, Aiken AH, et al. Presyrinx in children with chiari malformations. Neurology 2008;71:351–6.
47. Chiapparini L, Saletti V, Solero CL, et al. Neuroradiological diagnosis of chiari malformations. Neurol Sci 2011;32(Suppl 3):S283–6.
48. Baisden J. Controversies in chiari I malformations. Surg Neurol Int 2012;3:S232–7.
49. Currarino G. Canalis basilaris medianus and related defects of the basiocciput. AJNR Am J Neuroradiol 1988;9:208–11.
50. Beltramello A. Fossa navicularis magna. AJNR Am J Neuroradiol 1998;19:1796–8.
51. Hemphill M, Freeman JM, Martinez CR, et al. A new, treatable source of recurrent meningitis: basioccipital meningocele. Pediatrics 1982;70:941–3.
52. Central Brain Tumor Registry of the United States. Statistical report: primary brain tumors in the United States, 1997–2001. Hinsdale (IL): Central Brain Tumor Registry of the United States. 2015.
53. McMaster ML, Goldstein AM, Bromley CM, et al. Chordoma: incidence and survival patterns in the United States, 1973–1995. Cancer Causes Control 2001;12:1–11.
54. Mizerny BR, Kost KM. Chordoma of the cranial base: the McGill experience. J Otolaryngol 1995; 24:14–9.
55. Dorfman HD, Czerniak B. Bone cancers. Cancer 1995;75:203–10.
56. Mindell ER. Chordoma. J Bone Joint Surg Am 1981; 63:501–5.
57. Menezes AH, Traynelis VC. Tumors of the craniocervical junction. In: Youmans JR, editor. Neurological surgery. 4th edition. Philadelphia: Saunders; 1996. p. 3041–72.
58. Lanzino G, Sekhar LN, Hirsch WL, et al. Chondromas and chondrosarcomas involving the cavernous sinus: review of surgical treatment and outcomes in 31 patients. Surg Neurol 1993;40:359–71.
59. Borba LA, Al-Mefty O, Mrak RE, et al. Cranial chordoma in children and adolescents. J Neurosurg 1996;84:584–91.
60. Erdem E, Angtuaco EC, Van Hemert R, et al. Comprehensive review of intracranial chordoma. Radiographics 2003;23:995–1009.
61. Mehnert F, Beschorner R, Kuker W, et al. Retroclival ecchordosis physaliphora: MR imaging and review of the literature. AJNR Am J Neuroradiol 2004;25:1851–5.
62. Srinivasan A. Case 133: Ecchordosis Physaliphora. Radiology 2008;247(2):585–8.
63. Heffelfinger MJ, Dahlin DC, MacCarty CS, et al. Chordomas and cartilaginous tumors of the skull base. Cancer 1973;32:410–20.
64. Korten AG, ter Berg HJ, Spincemaille GH, et al. Intracranial chondrosarcoma: review of the literature and report of 15 cases. J Neurol Neurosurg Psychiatr 1998;65:88–92.
65. Meyers SP, Hirsch WL, Curtin HD, et al. Chondrosarcomas of the skull base: MR imaging features. Radiology 1992;184(1):103–8.
66. Yeom KW, Lober RM, Mobley BC, et al. Diffusion-weighted MRI: distinction of skull base chordoma from chondrosarcoma. AJNR Am J Neuroradiol 2013;34:1056–61. s1.
67. Leonard J, Gökden M, Kyriakos M, et al. Malignant giant-cell tumor of the parietal bone: case report and review of the literature. Neurosurgery 2001; 48(2):424–9.
68. Saleh EA, Taibah AK, Naguib M, et al. Giant cell tumor of the lateral skull base: a case report. Otolaryngol Head Neck Surg 1994;111(3 Pt 1):314–8.
69. Pitkethly DT, Kempe LG. Giant cell tumor of the sphenoid. Report of two cases. J Neurosurg 1994; 80:148–51.
70. Bertoni F, Unni KK, Beabout JW, et al. Giant cell tumor of the skull. Cancer 1992;70(5):1124–32.
71. Du Preez JH, Branca EP. Plasmacytoma of the skull: case reports. Neurosurgery 1991;29:902–6.
72. Benli K, Inci S. Solitary dural plasmacytoma: case report. Neurosurgery 1995;36:1206–9.
73. Romano AJ, Shoemaker EI, Gado M, et al. Neuroradiology case of the day: plasmacytoma of the skull vault. AJR Am J Roentgenol 1989;152(6): 1335–7.

74. Provenzale JM, Schaefer P, Traweek ST, et al. Craniocerebral Plasmacytoma: MR Features. AJNR Am J Neuroradiol 1997;18:389–92.
75. Vogl TJ, Steger W, Grevers G, et al. MR characteristics of primary extramedullary plasmacytoma in the head and neck. AJNR Am J Neuroradiol 1996;17:1349–54.
76. Tabareau-Delalande F, Collin C, Gomez-Brouchet A, et al. Diagnostic value of investigating GNAS mutations in fibro-ossous lesions: a Retrospective study of 91 cases of fibrous dysplasia and 40 other fibro-osseous lesions. Mod Pathol 2013;26(7):911–21.
77. Windholz F. Osteoporosis Circumscripta Cranii: its pathogenesis and occurrence in Leontiasis Osseaand in hyperparathyroidism. Radiographics 1945;44(1):14–22.